Supplementary Materials for

Mapping the spatiotemporal continuum of structural connectivity development across the human connectome in youth

Xiaoyu Xu[1,2,3], Hang Yang[2,3], Jing Cong[1,2,3], Haoshu Xu[2,3,4], Jason Kai[5], Shaoling Zhao[2,3], Yang Li[2,3], Kangcheng Wang[6], Valerie J. Sydnor[7], Ting Xu[5], Fang-Cheng Yeh[8], Zaixu Cui[2,3*]

*Correspondence: cuizaixu@cibr.ac.cn

Supplemental information

Supplementary Text

Methods of sensitivity analyses

We conducted sensitivity analyses to show that the developmental variability was robust to methodological choices, including 1) varying the number of sensorimotor-association (S-A) cortical systems; 2) reconstructing structural connectomes using the canonical Yeo-7 and Yeo-17 cortical parcellations; 3) rebuilding connectomes from major bundle-based TractSeg tractography; 4) regressing out Euclidean distance between system pairs when assessing S-A alignment; 5) including socioeconomic status (SES) and intracranial volume (ICV) as additional covariates; and 6) defining an alternative S-A connectional axis based on the product of system ranks. The developmental analyses were replicated using the HCP-D dataset. For each sensitivity analysis, we examined the alignments of second derivatives of developmental trajectories and age-resolved developmental slopes with the S-A connectional axis.

The first sensitivity analysis examined whether the scale of the large-scale structural connectome affected the results. Rather than parcellating the cortex into 12 cortical systems, we generated cortical parcellations with 7 or 17 systems defined along the S-A axis, ensuring each system contained approximately the same number of brain regions. We then reconstructed structural connectomes with 28 connections among 7 systems and 153 connections among 17 systems for each scan. Developmental models were refit for each connection in the HCP-D dataset.

Second, to assess robustness using canonical Yeo functional system parcellations[1], we constructed large-scale structural connectomes based on both the Yeo-7 and Yeo-17 systems, defined from the Schaefer-400 atlas. Consistent with our primary analysis, limbic regions were removed, resulting in 6 remaining systems for the Yeo-7 parcellation and 15 remaining systems for the Yeo-17 parcellation. The Yeo systems were ranked according to the average S-A cortical-axis rank of the brain regions within each system. The Yeo-7 connectome contained 21 undirected connections, while the Yeo-17 connectome contained 120 undirected connections. Developmental models were refit for each connection in the HCP-D dataset.

Third, we reconstructed the "global tractography" by merging 72 anatomically well-described bundles from TractSeg for each participant, which helped to minimize potential noise introduced by global tractography[2]. TractSeg is a convolutional neural network-based approach that accurately and rapidly segments tracts in individual spaces[3]. It segments white matter bundles and their end regions, which are then used for bundle-specific tractography. The structural connectomes reconstructed based on the major bundle-based tractography contains only long fibers belonging to the major tracts such as arcuate fascicle and corpus callosum. Specifically, we extracted the peaks of the constrained spherical deconvolution (CSD) function of white matter, identifying bundle start and end segmentations for all 72 bundles using TractSeg. These bundles were reconstructed using the iFOD2 algorithm, with an upper limit of 10k streamlines generated for each bundle. Consistent with the primary analysis, we constructed structural connectomes based on 12 systems along the S-A cortical axis. Structural connectivity strength was estimated by multiplying streamline counts by SIFT2 coefficients, normalized by the average volume of the paired systems. Streamlines belonging to connections with a coefficient of variation (CV) above the 75th percentile were excluded. Although this method excludes short regional u-fibers, which are biologically feasible, it significantly reduces potential noise from spurious fibers. We re-estimated the developmental models for connections derived from the major bundle-based tractography to test whether the observed developmental variability along the S-A axis was influenced by tractography noise.

Fourth, because Euclidean distance between regions can influence the developmental

patterns of structural connections, we evaluated whether this distance might confound our findings. Specifically, we regressed the Euclidean distance between each pair of systems in MNI space out of the average second derivatives of developmental trajectories and age-resolved developmental slopes. We then repeated the analyses examining the alignment of these metrics with the S-A connectional axis.

Fifth, we tested whether our findings were confounded by SES or ICV. SES was measured using the family income-to-needs ratio, as in prior work[4,5]. The family income-to-needs ratio was calculated as annual family income divided by the federal poverty threshold, as defined by the U.S. Department of Health and Human Services (https://aspe.hhs.gov/topics/poverty-economic-mobility/poverty-guidelines/prior-hhs-poverty-guidelines-federal-register-references). Intracranial volume was computed via *FreeSurfer*. We refitted the developmental models for each connection while additionally controlling for the participants' SES or ICV.

Sixth, in the primary analyses, we defined the S-A connectional-axis rank of each edge as the squared sum of the S-A cortical-axis ranks of the connected systems. To demonstrate that developmental patterns of structural connections are consistent across alternative definitions of the S-A connectional axis, we instead defined this rank as the product of the S-A cortical-axis ranks of each pair of systems (**Fig. S6a**). Under this alternative definition, connections between intermediate-level areas are assigned higher ranks than connections between the most sensorimotor and most transmodal association regions. We then repeated the developmental analyses using this alternative definition.

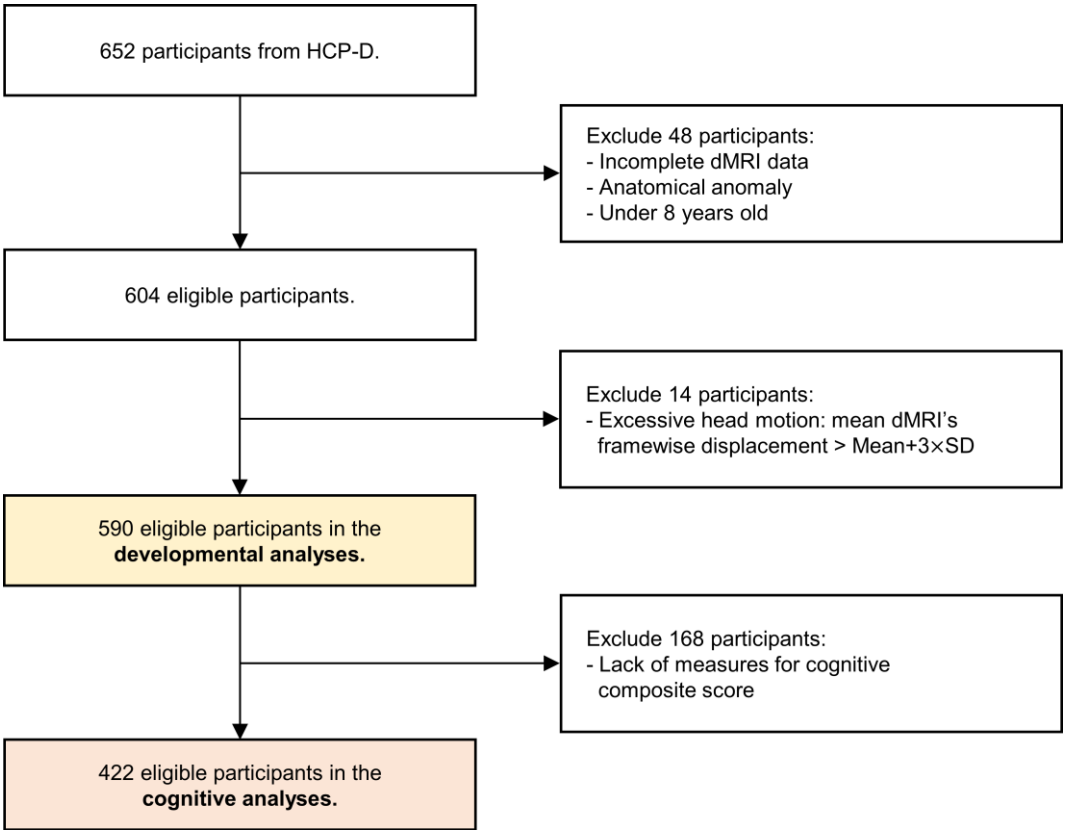

Fig. S1. Flowchart of inclusion and exclusion for participants in the HCP-D dataset. HCP-D: the Lifespan Human Connectome Project Development; dMRI: diffusion magnetic resonance imaging; SD: standard deviation.

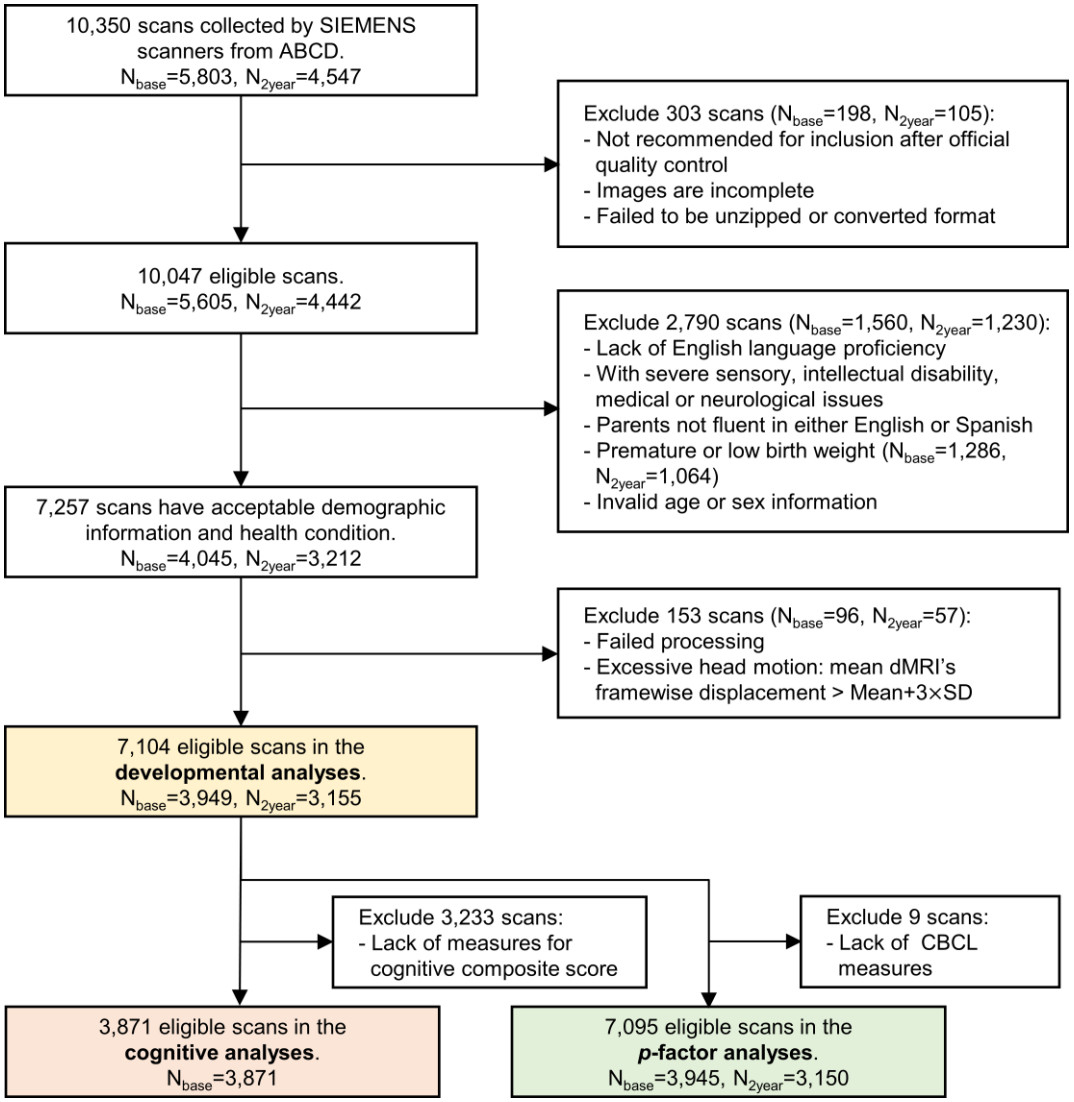

Fig. S2. Flowchart of inclusion and exclusion for participants in the ABCD dataset. ABCD: the Adolescent Brain Cognitive Development; CBCL: Child Behavior Checklist.

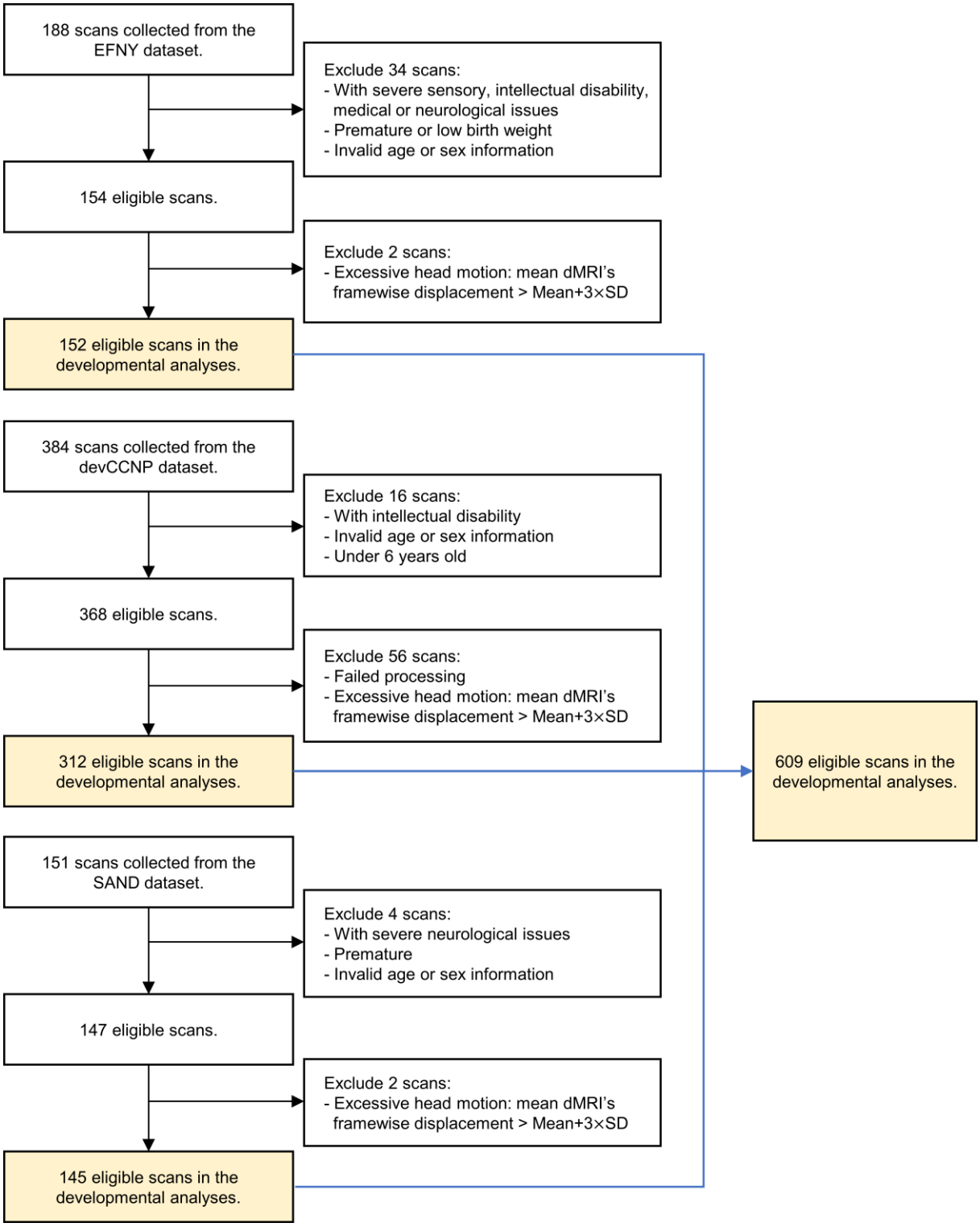

Fig. S3. Flowchart of inclusion and exclusion for participants in the Chinese Cohort dataset. devCCNP: the developmental component of the Chinese Color Nest Project; EFNY: Executive Function and Neurodevelopment in Youth; SAND: Shandong Adolescent Neuroimaging Project on Depression.

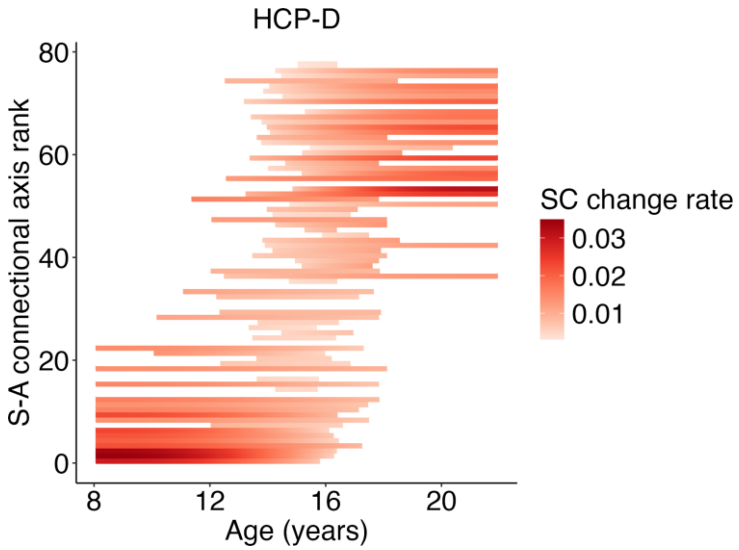

Fig. S4. Significant developmental rates of the large-scale structural connections in the HCP-D dataset. The rate of developmental changes of the large-scale structural connections were measured using the first derivatives at 1,000 age points evenly sampled from the age range of 8.1 to 21.9 years. Each row represents an edge, with colors coded based on the magnitudes and direction of the significant developmental rates ($P_{FDR} < 0.05$). Insignificant developmental rates are shown in white. Since all significant derivatives are above zero, we used different shades of red to indicate their magnitudes. SC: structural connectivity; S-A: sensorimotor-association.

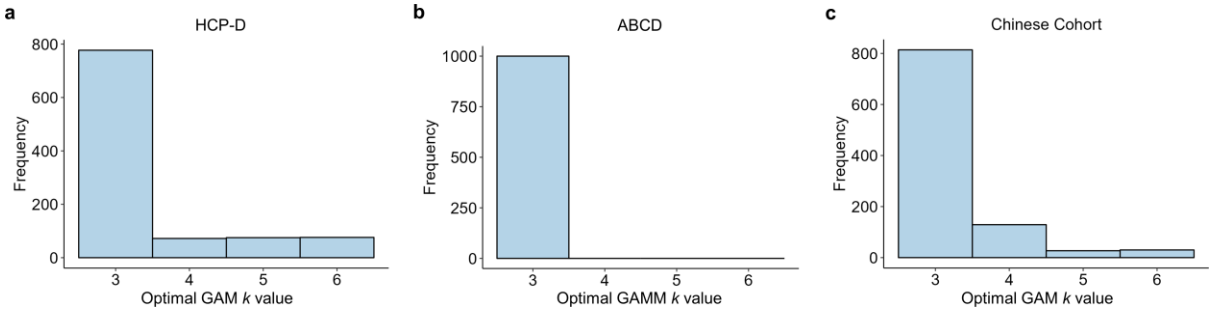

Fig. S5. Selection frequency of *k* values across bootstrap iterations. Across 1,000 iterations, a *k* value of 3 was selected as the optimal choice in 777 iterations for the HCP-D dataset (**a**), 1,000 iterations for the ABCD dataset (**b**), 814 iterations for the Chinese Cohort dataset (**c**).

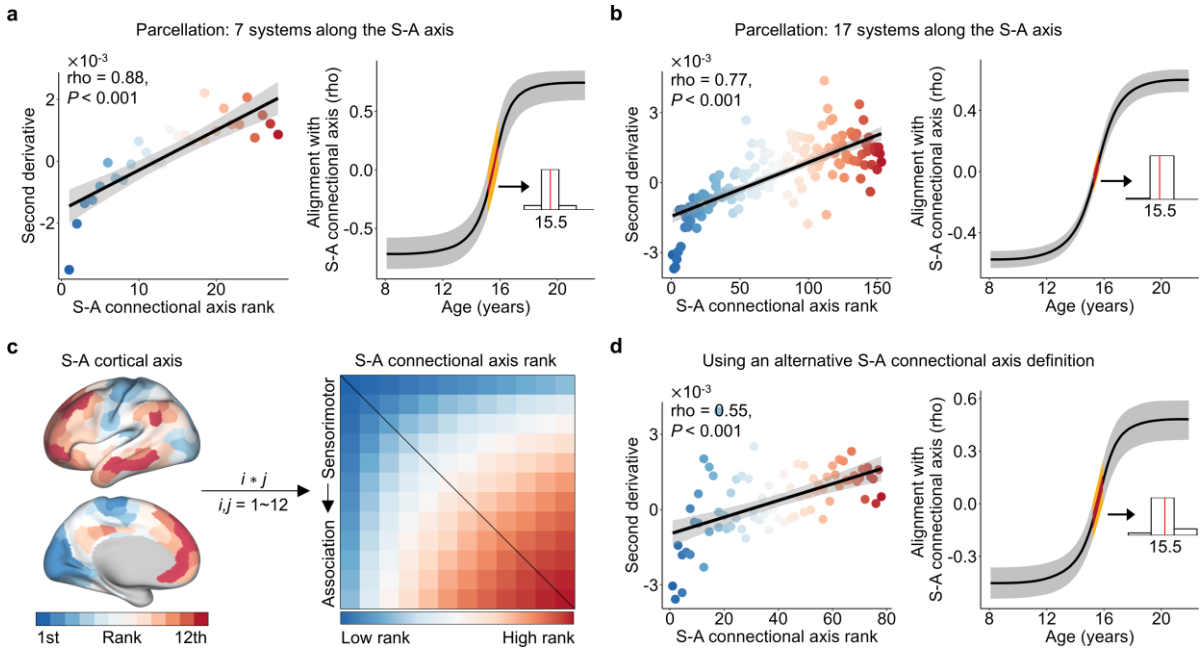

Fig. S6. Sensitivity analyses using alternative network scales and S-A connectional axis definition. We first replicated the key results using structural connectomes with alternative network scales of 7 (**a**) and 17 (**b**). For each scale, the left panel shows the second derivatives of developmental trajectories are strongly correlated with the S-A connectional axis ranks. The right panel shows the age-resolved alignment between the spatial pattern of structural-connectivity development slopes and the S-A axis; the yellow band marks the age window of zero alignment, with the median age annotated. **c**, Then, we defined the S-A connectional axis by multiplying the S-A cortical axis ranks of each pair of nodes. **d**, The second derivatives remained correlated with the S-A connectional axis ranks (rho = 0.55, $P < 0.001$). The alignment between the spatial pattern of structural connectivity development and the S-A connectional axis evolves throughout youth with a zero-alignment occurred at 15.5 years. S-A: sensorimotor-association.

Table S1. Demographic and cognitive characteristics of participants from the HCP-D dataset.

	HCP-D dataset
N	590
Age (years) (mean (SD))	14.72 (3.92)
Sex = Male (%)	273 (46.3)
Handedness (%)	
Right-handed	519 (88.0)
Left-handed	43 (7.3)
Mixed handed	28 (4.7)
Race/ethnicity (%)	
Hispanic	86 (14.6)
Non-Hispanic Asian	43 (7.5)
Non-Hispanic Black	56 (9.5)
Non-Hispanic White	344 (58.3)
Others	61 (10.3)
Average cognitive performance (mean (SD))	107.76 (12.75)
Mean FD (mean (SD))	0.66 (0.20)
Sites (%)	
Harvard	198 (33.6)
UMinn	156 (26.4)
UCLA	105 (17.8)
WashU	131 (22.2)
Intracranial volume (mm^3) (mean (SD))	1598201.51 (154010.77)
Family income-to-needs ratio	5.48 (6.04)

Note: The number of participants and percentages were displayed for categorical variables, while mean and standard deviation (SD) were provided for numeric variables. Ages in months and sex were extracted from 'HCD_LS_2.0_subject_completeness.csv' in the HCP-D dataset. Ages were converted to years by dividing by 12. Handedness scores derived from 'edinburgh_hand01.txt' were converted into a 3-level factor. Scores over 60 were defined as right-handed, under -60 as left-handed, and those in the middle as mixed-handed[6]. Race was obtained from 'socdem01.txt'. Average cognitive performance without age correction were derived from 'cogcomp01.txt'. Mean framewise displacement (FD) measures head motion during diffusion MRI scanning[7]. Site information was derived from 'ndar_subject01.txt'. The family income-to-needs ratio was calculated by dividing the annual family income ('socdem01.txt') by the federal poverty line for the year of the interview and the family size.

Table S2. Demographic, cognitive, and psychiatric characteristics of participants in the ABCD dataset.

	Baseline	Two-year follow-up
N	3949	3155
Age (years) (mean (SD))	9.93 (0.63)	11.95 (0.65)
Sex = male (%)	2075 (52.5)	1701 (53.9)
Race/ethnicity (%)		
Hispanic	678 (17.2)	525 (16.6)
Non-Hispanic Asian	68 (1.7)	41 (1.3)
Non-Hispanic Black	575 (14.6)	476 (15.1)
Non-Hispanic White	2257 (57.2)	1817 (57.6)
Other	371 (9.4)	296 (9.4)
Handedness (%)		
Right-handed	3166(80.2)	2510(79.6)
Left-handed	270(6.8)	230(7.3)
Mixed handed	513(13.0)	415(13.2)
Average cognitive performance (mean (SD))	92.53 (10.12)	-
P-factor (mean (SD))	0.07(0.83)	0.04(0.82)
Mean FD (mean (SD))	0.55 (0.21)	0.53 (0.20)
Sites (%)		
Site02	174(4.4)	161(5.1)
Site03	308(7.8)	248(7.9)
Site05	225(5.7)	183(5.8)
Site06	392(9.9)	314(10.0)
Site07	153(3.9)	123(3.9)
Site09	258(6.5)	162(5.1)
Site11	268(6.8)	190(6.0)
Site12	444(11.2)	317(10.0)
Site14	241(6.1)	176(5.6)
Site15	204(5.2)	168(5.3)
Site16	696(17.6)	581(18.4)
Site20	219(5.5)	226(7.2)
Site21	367(9.3)	306(9.7)
Intracranial volume (mm^3) (mean (SD))	1534157.62(132994.37)	1561853.71(140683.69)
Family income-to-needs ratio	3.80(2.35)	3.81(2.29)

Note: The number of participants and percentages were displayed for categorical variables, while mean and SD were displayed for numeric variables. Ages in months and site information were obtained from 'abcd_y_lt.csv'. Ages were then converted to years by dividing by 12. Sex and race/ethnicity were extracted from 'abcd_p_demo.csv'. Three-factor handedness was acquired from 'nc_y_ehis.csv'. Average cognitive performance without age correction were obtained from 'nc_y_nihtb. csv'. General psychopathology factor (*p*-factor) scores were

derived from the CBCL. The family income-to-needs ratio was calculated by dividing the annual family income (‘abcd_p_demo. csv’) by the federal poverty line for the year of the interview and the family size.

Table S3. Demographic and cognitive characteristics of participants from the Chinese Cohort dataset.

	devCCNP-ses1	devCCNP-ses2	devCCNP-ses3	EFNY	SAND
N	210	73	29	152	145
Age (years) (mean (SD))	9.68 (2.60)	10.85 (2.34)	12.17 (2.10)	11.70 (3.62)	15.54 (3.24)
Sex = male (%)	120 (57.1)	41 (56.2)	20 (69.0)	85 (55.9)	51 (35.2)
Race (%)					
Asian	210 (100.0)	73 (100.0)	29 (100.0)	152 (100.0)	145 (100.0)
Handedness (%)					
Right-handed	184 (93.4)	70 (97.2)	29 (100.0)	109 (71.7)	101 (78.9)
Left-handed	5 (2.5)	1 (1.4)	0 (0.0)	2 (1.3)	0 (0.0)
Mixed handed	8 (4.1)	1 (1.4)	0 (0.0)	41 (27.0)	27 (21.1)
Mean FD (mean (SD))	0.59 (0.34)	0.49 (0.27)	0.41 (0.17)	0.57 (0.12)	0.59 (0.19)
Intracranial volume (mm^3) (mean (SD))	1450508.93 (134656.16)	1493327.38 (132939.62)	1590492.17 (157471.04)	1541783.89 (146595.36)	1427493.68 (216870.43)

Note: The number of participants and percentages were displayed for categorical variables, while mean and SD were provided for numeric variables. The demographic information from the devCCNP was obtained from the participant information table. The demographic information of the EFNY and SAND was provided by Z.C., Y.L. and K.W.

Table S4. Image acquisition parameters for T1-weighted images and diffusion MRI for each dataset.

	Sequence	TR (ms)	TE (ms)	TI (ms)	Flip angle (°)	FOV (mm^2)	Slices	Voxel Size (mm)	Diffusion directions	b-values (s/mm^2)	Acquisition time (min:s)
HCP-D (3T SIEMENS Prisma with 32-channel head coil)											
T1WI	MPRAGE	2500	1.8,3.6, 5.4,7.2	1000	8	256×256	208	0.8	NA	NA	8:22
dMRI (AP/PA)	Multiband EPI	3230	89.2	NA	78	210×210	92	1.5	185	1500, 3000	5:37*2runs* 2sessions
ABCD (3T SIEMENS)											
T1WI	MPRAGE	2500	2.88	1060	8	256×256	176	1.0	NA	NA	7:12
dMRI (PA)	Multiband EPI	4100	88	NA	90	240×240	81	1.7	96	500, 1000, 2000, 3000	7:31
fmap (AP)	Single-band EPI	12400	89	NA	90	240×240	81	1.7	0	0	Not available
Chinese Cohort-EFNY (3T SIEMENS Prisma with 64-channel head coil)											
T1WI	MPRAGE	1500	1.87	756	10	256×256	208	0.8	NA	NA	7:15
dMRI (PA)	Multiband EPI	3100	86	NA	90	205×205	84	1.8	120	500, 1000, 2000, 3000	7:00
fmap (AP)	Multiband EPI	3100	86	NA	90	205×205	84	1.8	0	0	0:32
Chinese Cohort-devCCNP (3T GE discovery MR750 with 8-channel head coil)											
T1WI	3D SPGR	6.7	2.9	450	12	256×256	176	1.0	NA	NA	4:41
dMRI (PA)	Single-band EPI	8724	81.4	NA	90	224×224	75	2.0	64	1000	10:54

Table S4 (continued). Image acquisition parameters for T1-weighted images and diffusion MRI for each dataset.

	Sequence	TR (ms)	TE (ms)	TI (ms)	Flip angle (°)	FOV (mm^2)	Slices	Voxel Size (mm)	Diffusion directions	b-values (s/mm^2)	Acquisition time (min:s)
Chinese Cohort-SAND (3T SIEMENS Verio)											
T1WI	MPRAGE	2400	2.2	1000	8	256×256	208	0.9	NA	NA	Not available
dMRI (AP)	Single-band EPI	9635	100	NA	90	256×256	66	2	64	1000	Not available

Note: T1WI: T1-weighted imaging; dMRI: diffusion magnetic resonance imaging; MPRAGE: magnetization prepared rapid gradient echo; EPI: echo planar imaging; 3D SPGR: three-dimensional spoiled gradient recalled; AP: anterior-to-posterior phase-encoding direction; PA: posterior-to-anterior phase-encoding direction.

References

1 Yeo, B. T. *et al.* The organization of the human cerebral cortex estimated by intrinsic functional connectivity. *J Neurophysiol* **106**, 1125-1165 (2011). https://doi.org/10.1152/jn.00338.2011

2 Yeh, F. C. Population-based tract-to-region connectome of the human brain and its hierarchical topology. *Nat Commun* **13**, 4933 (2022). https://doi.org/10.1038/s41467-022-32595-4

3 Wasserthal, J., Neher, P. & Maier-Hein, K. H. TractSeg - Fast and accurate white matter tract segmentation. *NeuroImage* **183**, 239-253 (2018). https://doi.org/10.1016/j.neuroimage.2018.07.070

4 Barch, D. M. *et al.* Early Childhood Socioeconomic Status and Cognitive and Adaptive Outcomes at the Transition to Adulthood: The Mediating Role of Gray Matter Development Across Five Scan Waves. *Biological Psychiatry: Cognitive Neuroscience and Neuroimaging* **7**, 34-44 (2022). https://doi.org/https://doi.org/10.1016/j.bpsc.2021.07.002

5 King, L. S., Dennis, E. L., Humphreys, K. L., Thompson, P. M. & Gotlib, I. H. Cross-sectional and longitudinal associations of family income-to-needs ratio with cortical and subcortical brain volume in adolescent boys and girls. *Developmental cognitive neuroscience* **44**, 100796 (2020).

6 Edlin, J. M. *et al.* On the use (and misuse?) of the Edinburgh Handedness Inventory. *Brain Cogn* **94**, 44-51 (2015). https://doi.org/10.1016/j.bandc.2015.01.003

7 Power, J. D. *et al.* Methods to detect, characterize, and remove motion artifact in resting state fMRI. *NeuroImage* **84**, 320-341 (2014). https://doi.org/https://doi.org/10.1016/j.neuroimage.2013.08.048